

## **Thermal Conductivity of Trinidad ‘Guanapo Sharp Sand’**

Krishpersad Manohar, Lecturer, Mechanical and Manufacturing Engineering Department, The University of the West Indies, St. Augustine, Trinidad, West Indies. Email: [kmanohar@eng.uwi.tt](mailto:kmanohar@eng.uwi.tt)

Kimberly Ramroop, M.Phil. Candidate, Mechanical and Manufacturing Engineering Department, The University of the West Indies, St. Augustine, Trinidad, West Indies.

Gurmohan S. Kochhar, Professor, Department of Mechanical & Manufacturing Engineering, The University of the West Indies, St. Augustine, Trinidad, West Indies. Email: [guru@eng.uwi.tt](mailto:guru@eng.uwi.tt)

### **ABSTRACT**

The thermal conductivity variation of “sharp sand” with moisture and grain size was investigated using a thermal probe method. The probe used for testing was built in accordance with ASTM D 5334 and calibrated using heat-flow meter data. Calibration tests demonstrated repeatability  $\pm 3.5\%$  for a 95% confidence of the  $dT/d \ln t$  slope. Experiments were conducted on two sand specimens with grain size ranging from  $150\mu\text{m}$  to  $300\mu\text{m}$  (fine) and  $301\mu\text{m}$  to  $600\mu\text{m}$  (coarse). Test density was maintained at approximately  $1400 \text{ kg/m}^3$  for each specimen and data were recorded for specimens with 0%, 2.5%, 5% and 7.5% wt.% water. The experimental results showed a well defined increase in  $\lambda$  with water content for both specimens. The fine sand has a more rapid increase in  $\lambda$  with water content than the coarse sand.

### **NOMENCLATURE**

n	Number of data points in chosen time interval	
Q	Power emitted by probe per unit length	(W/m)
R	Electrical resistance	( $\Omega$ )

$r$	Radial distance from probe	(mm)
$T$	Temperature	(°C)
$T_0$	Initial temperature	(°C)
$t$	Time	(s)
$V$	Voltage	(V)
$V$	Volume	(m <sup>3</sup> )
$W$	Weight	(kg)
$\kappa$	Thermal diffusivity	(m <sup>2</sup> /s)
$\lambda$	Apparent thermal conductivity	(W/m.K)

## 1. INTRODUCTION

Sand and granular material are commonly used as protective shock-absorbing material around pipelines and underground cables. A layer of backfill granular material gives stability and serves as a protection by allowing for some movement. In many cases, however, the thermal properties of the material are of significant importance as electrical cables need to dissipate the internally generated heat and gas and steam lines may be affected by the heat gain or loss from the surroundings.

The thermal characteristics of the backfill material and the variation with moisture will determine the extent of the thermal influence. The thermal properties of granular material are influenced by the water content, pore space and packing density. Compared to air, water has a high thermal conductivity, hence, a small amount of distributed water will significantly affect the thermal conductivity. Grain size and packing density have an effect on the solid-phase conduction.

## **2. SAND TYPE**

The material selected for this study was Guanapo Sand, locally known as ‘sharp sand’. This material is readily available at the Turure National Quarries Plant, Trinidad, West Indies, and is found as terrace deposits and river gravel in the northern basin of Trinidad. Guanapo Sand is a well-characterized material with a slight yellow color that consists of 98% silica and traces of iron oxide.

From randomly selected samples, two different grain size range were obtained. A mechanical shaker was used to separate particles passing a 300  $\mu\text{m}$  sieve but retained on a 150  $\mu\text{m}$  sieve defined the fine sand specimen. This material is described as a fine sand with sub-angular and sub-rounded grains. Particles passing a 600  $\mu\text{m}$  sieve but retained on a 300  $\mu\text{m}$  sieve made up the coarser grain specimen. This material is described as medium sand with sub-angular and sub-rounded grains [1].

## **3. SPECIMEN CONDITIONING**

The graded sand samples were dried in a dehumidifying chamber at 50°C to avoid any micro-structural changes. Test specimens were weighed at 24 h intervals until no change in weight was observed. This condition was taken as zero percent water content and used as the datum for wt.% water.

## **4. TEST SPECIMEN SIZING**

From the theory of the continuous line source heater [2, 3], Equation 1 is the approximate solution for the temperature variation with time in an infinite solid, initially at temperature  $T_0$ , heated by a line source.

$$T - T_0 = (Q/4\pi\kappa)\ln(4\kappa t/r^2) - 0.5772(Q/4\pi\kappa) \quad (1)$$

Using a specific heat and thermal conductivity estimate of 0.796 kJ/kg.K and 2 W/m.K, respectively, for a density of 1400 kg/m<sup>3</sup> [4, 5], the radial distance  $r$  at which  $T - T_0$  is zero after 1000 s was calculated to be 65 mm. Therefore, for all practical purposes, cylindrical specimens of radius 150 mm radius represented an infinite medium with respect to a line source heater over a test time of 1000 s.

## 5. SAMPLE PREPARATION

Sand specimens 200 mm deep were used to ensure that when the 100 mm probe was fully inserted to represent the line source, end effects would be negligible. The weight,  $W$ , of dry sand for each specimen was calculated from the volume,  $V$ , of the sand in cubic meters.

$$W = V \times 1400 \quad (2)$$

For the dry sand specimens the weighed sand was uniformly packed in the cylindrical container to the 200 mm height to produce the approximate target density of 1400 kg/m<sup>3</sup>.

For the wet sand specimens, the respective mass of dry sand was mixed with the mass of water required to give the necessary moisture content. The water and sand were mixed manually to form a homogeneous mixture. Test specimens were re-weighed after mixing to ensure the correct water content. The wet sand was then packed into the cylindrical test containers to the required depth such that a density of 1400 kg/m<sup>3</sup> was achieved. For each grain size five test specimens were prepared with 0, 2.5, 5.0 and 7.5 wt.% water. For 10 wt.% water the test specimens drained

off excess water showing that the sand was water saturated between 7.5 to 10 wt.% water.

## **6. THERMAL PROBE**

The thermal probe used to represent a line source was constructed from seamless thin-walled stainless steel tubes, 100 mm long and 3 mm outer diameter (Figure 1). The main probe components are a manganin wire heater and a thermocouple [3]. The probe assembly is described in ASTM D 5334 [6].

Insulated manganin heater wire, 0.358 mm in diameter, was looped and inserted into the full length of the tube to form the heating element and a 30 gage T-type thermocouple was inserted midway along the length of the tube. Both ends of the heating element and the thermocouple wires protruded from the same end of the tube and were passed through a nylon cap. Following the procedure described in ASTM D 5334 [6], the tube was filled with a clear plastic epoxy resin and a metal tip was placed on the open end of the tube. The epoxy was allowed 24 h setting time and the extended heater wire ends were cut close to the thermal probe and power supply leads were soldered to them.

## **7. DATA ACQUISITION**

The temperature-time variation of the T-type thermocouple in the thermal probe was monitored and recorded using the Pico TC-08 data-logger with a RS-232 computer interface. Figure 2 shows a schematic of the experimental set-up. The data-logger provided internal electronic compensation for the thermocouple. The computer was programmed to sense ten temperature signals per second, compute

the average and display it each second, store and display readings of time and temperature for a total of 1000 entries. The EXTECH DC Regulated Power Supply was used to energize the probe and maintain a constant voltage and current during testing.

## **8. THEORY – $\lambda$ MEASUREMENT**

The solution for the temperature variation with time of a cylinder of a perfect conductor with small radius that is transmitting heat at a constant rate to the surrounding isothermal infinite medium with constant properties indicates that a plot of temperature against  $\ln t$  has a linear asymptote, with slope  $(Q/4\pi\lambda)$  [2]. Therefore, if the value of  $Q$  is known then the apparent thermal conductivity  $\lambda$  is determined from Equation (3).

$$\lambda = \frac{(Q/4\pi)}{(dT/d \ln t)} \quad (3)$$

In practical situations, however, the finite radius and mass of the probe results in a time delay before the rate of radial heat flow across the surface of the probe is equal to the heat generated by the manganin filament [7]. Therefore, for practical situations, the general shape of the  $T - \ln t$  plot includes an initial nonlinear region that is followed by a linear region. With the passage of time, the probe temperature will level off to a steady-state value as the rate of heat dissipated through the sand at the probe surface is the same as the heat generated in the probe.

## 9. EXPERIMENTAL UNCERTAINTY

The experimentally determined  $\lambda$  is calculated from Equation (3) in which  $\lambda$  is proportional to the ratio of  $Q/(dT/d \ln t)$ . The value of  $Q$  depends on the product of a voltage and current reading.  $dT / d \ln t$  is the slope  $b$  of the  $T$ - $\ln t$  curve. From the theory of uncertainty analysis [8], the square of the uncertainty in the experimentally determined  $\lambda$  is given by Equation (4).

$$\left(\frac{\Delta\lambda}{\lambda}\right)^2 = \left(\frac{\Delta V}{V}\right)^2 + \left(\frac{\Delta I}{I}\right)^2 + \left(\frac{\Delta b}{b}\right)^2 \quad (4)$$

where  $\frac{\Delta\lambda}{\lambda}$ ,  $\frac{\Delta V}{V}$ ,  $\frac{\Delta I}{I}$ , and  $\frac{\Delta b}{b}$  are the uncertainties in experimentally determined  $\lambda$ , voltage, current, and slope, respectively.

The EXTECH micro-controller based DC power supply displayed voltage readings up to  $10^{-2}$  with a limiting error of  $\pm 6$  mV in the 0 – 30 volts range [9]. The power supply displayed current readings up to  $10^{-2}$  with a limiting error of  $\pm 5$  mA in the range 0 – 3 amps range. From Equation (4) the square of the uncertainty associated with the measured  $\lambda$  is

$$\begin{aligned} \left(\frac{\Delta\lambda}{\lambda}\right)^2 &= \left(2\frac{6 \times 10^{-3}}{30}\right)^2 + \left(2\frac{5 \times 10^{-3}}{3}\right)^2 + \left(\frac{\Delta b}{b}\right)^2 \\ &= 1.6 \times 10^{-7} + 1.1 \times 10^{-5} + \left(\frac{\Delta b}{b}\right)^2 \end{aligned}$$

In comparison to the range of values associated with measured  $\lambda$ , the uncertainty of the sum of voltage and current is small. Hence, the uncertainty of  $\lambda$  is characterized by the uncertainty in the slope  $b$  of the straight line fit to the experimental data.

## 10. EXPERIMENTAL PROCEDURE

The thermal probe was used to test sand specimens in the laboratory. The analysis based on Equation (1) required that the test specimen be isothermal, thus limiting in situ usage. The experimental procedure involved inserting the probe in the material to be tested after both were in thermal equilibrium with the surroundings. Since the friction associated with inserting the probe may cause a measurable temperature increase, the probe temperature was monitored to make certain that isothermal conditions were attained before the heater was powered. This thermal equilibration usually took 10 to 15 min.

The data acquisition system and heater power were turned on together once thermal equilibrium had been achieved. The data acquisition system recorded probe current, temperature, and time for approximately 1000 s. Since manganin wire has a negligible change in electrical resistance with temperature [10], the power to the probe heater remained constant.

A properly configured test could be completed with about 1000 s of data collection. Within this time limit, the  $T-\ln t$  variation of the probe should have the three distinct segments. The  $T-\ln t$  curve leveling off too soon ( $< 800$  s) was an indication that the power supplied was too low in which case thermal equilibrium at the probe surface was quickly achieved. This resulted in the linear section of the plot being too brief for analysis and the temperature increase too small for reliable results. A rapid increase in probe temperature was an indication that the power supplied to the heater was too high as the rate of heat dissipation through the sand was much lower than the rate of heat generation in the probe. This can cause heat build-up in the probe resulting in damage [5] and for materials with moisture, a



large rapid temperature gradient could result in moisture vaporization, causing a change in material properties [11]. The power was adjusted up or down to satisfy the test design time of 1000 s as recommended by ASTM D 5334 [6].

## 11. TEST DESIGN CRITERIA

The theory associated with determining apparent thermal conductivity from the T-ln t plot of the thermal probe (Equation 3) makes use of the slope associated with the linear segment of the heat-up curve. A least-square fit to a linear expression for T in terms of ln t was used to describe this segment of the heat-up curve. The analysis involves determining the slope for candidate intervals of 0 to 1000 s, 50 to 950 s, 100 to 900 s etc. The linear segment was taken to be such that three consecutive calculations of the slope differed by no more than 2.5%. The slope,  $dT / d \ln t$ , of the best-fit line for the data points within the selected time intervals was calculated using Equation 5 [12].

$$\frac{dT}{d \ln t} = \frac{n \sum (\ln t)(T) - (\sum \ln t)(\sum T)}{n \sum (\ln t)^2 - (\sum \ln t)^2} \quad (5)$$

This equation returns the slope of the linear regression line through the selected data points. The experimentally determined value for  $\lambda$  is directly proportional to  $d \ln t / dT$  which is the result of an analysis of (T, ln t) data. A standard statistical technique [12] was used to estimate the 95% confidence interval of this slope for the data points within the selected time interval.

## 12. CALIBRATION

The thermal probe used in this study was calibrated with commercially available fine cryogenic perlite as the reference material. Using a specific heat estimate of 1.005 kJ/kg.K for 51 kg/m<sup>3</sup> perlite at 31°C the radial distance,  $r$ , from Equation (1), at which  $(T - T_0)$  is zero after 1000 seconds is 43 mm. Therefore for all practical purposes, cylindrical specimens of radius 150 mm simulated an infinite medium over the test time of 1000 seconds. Eight calibration tests were conducted in accordance with the test design criteria. For each test the slope and  $\lambda$  values were determined using the procedure outlined above [3]. The linear region of the slope was selected in accordance with the 2.5% test design criterion. For a 95% confidence interval, the mean value for the slope, and  $\lambda$  for data that satisfied the test design conditions were calculated.

The calibration test results were compared with heat flow meter data for commercially available fine cryogenic perlite at 51 kg/m<sup>3</sup> [13]. The calibration test results showed a bias of 0.9542 when compared with heat flow meter data. Using the correction factor of 0.9542 the calibration test results against heat flow meter data demonstrated repeatability within  $\pm 3.5\%$  for a 95% confidence of the  $dT / d \ln t$  slope [3].

## 13. TEST RESULTS

For each of the two grain sizes, tests were conducted on specimens of 0, 2.5, 5.0 and 7.5 wt.% water. In each case data were logged for 1000 s, saved and exported to an excel spreadsheet. An excel program was used with the data to select a slope in accordance with the 2.5% criterion as in the probe calibration. Figure 3 show a

sample graph of the temperature In time variation over the 1000 s test period. The 95% confidence interval, the mean value for the slope, and  $\lambda$  for data that satisfied the 2.5% test design criterion were calculated. The probe correction factor of 0.9542 was applied to each test result and are shown in Tables 1 and 2. Table 3 lists some published data of sand and related material for comparison.

TABLE 1. EXPERIMENTAL TEST RESULTS - 150 $\mu$ m TO 300  $\mu$ m GRAIN SIZE (FINE)

Test	$\lambda$ at 0 wt.% water or 0 vol.% water (W/m.K)	$\lambda$ at 2.5 wt.% water or 3.5 vol.% water (W/m.K)	$\lambda$ at 5 wt.% water or 7 vol.% water (W/m.K)	$\lambda$ at 7.5 wt.% water or 10.5 vol.% water (W/m.K)
1	0.3456	0.7515	1.0939	1.2252
2	0.3454	0.7581	1.0385	1.2197
3	0.3409	0.7482	1.0812	1.1497
4	0.3462	0.7300	1.1236	1.2063
5	0.3320	0.7348	1.0924	1.1999
<b>Mean value</b>	<b>0.3420</b>	<b>0.7445</b>	<b>1.0859</b>	<b>1.2002</b>
<b>Std. Dev.</b>	<b>0.0060</b>	<b>0.0117</b>	<b>0.0308</b>	<b>0.0300</b>
<b>Coefficient of variation</b>	<b><math>\pm 1.8\%</math></b>	<b><math>\pm 1.6\%</math></b>	<b><math>\pm 2.8\%</math></b>	<b><math>\pm 2.5\%</math></b>

TABLE 2. EXPERIMENTAL TEST RESULTS - 301 $\mu$ m TO 600  $\mu$ m GRAIN SIZE (COURSE)

Test	$\lambda$ at 0 wt.% water or 0 vol.% water (W/m.K)	$\lambda$ at 2.5 wt.% water or 3.5 vol.% water (W/m.K)	$\lambda$ at 5 wt.% water or 7 vol.% water (W/m.K)	$\lambda$ at 7.5 wt.% water or 10.5 vol.% water (W/m.K)
1	0.3260	0.6604	0.8756	0.9113
2	0.3177	0.6269	0.8417	0.9368
3	0.3342	0.6571	0.8352	0.9338
4	0.3299	0.6320	0.8430	0.9188
5	0.3191	0.6294	0.8526	0.9158
<b>Mean value</b>	<b>0.3254</b>	<b>0.6412</b>	<b>0.8496</b>	<b>0.9233</b>
<b>Std. Dev.</b>	<b>0.0070</b>	<b>0.0162</b>	<b>0.0158</b>	<b>0.0113</b>
<b>Coefficient of variation</b>	<b><math>\pm 2.2\%</math></b>	<b><math>\pm 2.5\%</math></b>	<b><math>\pm 1.9\%</math></b>	<b><math>\pm 1.2\%</math></b>

TABLE 3. PUBLISHED DATA FOR SAND AND RELATED MATERIALS

<b>Material</b>	<b>Density (kg·m<sup>3</sup>)</b>	<b>Mean Test Temperature (°C)</b>	<b>Thermal Conductivity (W/m·K)</b>
Sand (dry) [15]	1518	20	0.325
Soil (dry) [15]	Not given	20	0.129
Soil and stones mixed (dry) [15]	2035	20	0.5193
All-purpose sand conditioned at 24 °C, 50% relative humidity.[3]	1730	30	0.52
Sifted sand conditioned at 24 °C, 50% relative humidity.[3]	1654	30	0.44
Soil (20.3 wt.% moisture) [3]	1893	30	2.11

## 14. DISCUSSION

Test results on sand at a density of approximately  $1400 \text{ kg/m}^3$  with grain size ranging between  $150 \text{ }\mu\text{m}$  to  $300 \text{ }\mu\text{m}$  (fine) and  $301 \text{ }\mu\text{m}$  to  $600 \text{ }\mu\text{m}$  (course) showed a decrease in thermal conductivity with increase in grain size. This is probably due to the larger void space associated with larger grain size. The smaller grain sand will pack closer forming a more homogenous specimen. The difference between the corresponding  $\lambda$  values for the fine and course sand at the respective wt.% (vol.%) water showed a progressive increase within the 0 to 7.5 wt.% water test range. The difference in  $\lambda$  between the fine and course sand at 0 wt.% water was about 5% which increased to 14%, 22% and 23% at 2.5 wt.% water, 5 wt.% water and 7.5 wt.% water, respectively. At 0 wt.% water both fine and course sand are essentially a homogenous mixture of sand grains and air. The  $\lambda$  is mainly influenced by the sand as air has a much lower thermal conductivity. With the addition of the same amount of distributed water within the smaller void spaces of the fine sand, a more homogenous water-sand mixture is formed compared to the course sand. This may have resulted in a consistently higher  $\lambda$  for the fine sand.

For both fine and course sand the apparent thermal conductivity increased with water addition. However, for even incremental increase in wt.% (vol.%) water the corresponding incremental increase in  $\lambda$  showed a progressive decline for both fine and course sand. The trend observed from Figure 4 indicated that  $\lambda$  approached a leveling off value as wt.% water increased. This trend can be attributed to the relatively high thermal conductivity water replacing the relatively low thermal conductivity air within the void spaces of the sand. As the distributed water content

increased and the void spaces filled with water the material became a homogenous mixture of water and sand. This trend and the  $\lambda$  range reported are consistent with published data [4,5,14] and the experimentally determined  $\lambda$  was within the range of published data listed in Table 3.

## **15. CONCLUSIONS**

- The apparent thermal conductivity ( $\lambda$ ) of sand with grain size 150 $\mu\text{m}$  to 300 $\mu\text{m}$  (fine) is higher than sand with grain size 301 $\mu\text{m}$  to 600 $\mu\text{m}$  (course).
- For 7.5 wt.% water the fine sand showed a 30% higher  $\lambda$  than the course sand.
- For even incremental increase in water content the corresponding incremental increase in  $\lambda$  gets smaller within the 0 to 7.5 wt.% range.
- Above 7.5 wt.% water the  $\lambda$  value tends to levels off.

## **16. WORK IN PROGRESS**

Testing on another grain size range is being conducted to look at the variation of  $\lambda$  with grain size at the respective percentage moisture content of 'sharp sand' and to develop a correlation for  $\lambda$  with grain size and moisture.



## 17. REFERENCES

1. Swanson, R. G.(1970). Sample Examination Manual. Methods in Exploration Series, The American Association of Petroleum Geologists, Tulsa, Oklahoma, USA, pp. IV-15 – IV-26.
2. Carslaw, H. S. and J. C. Jaeger. (1964). Conduction of Heat in Solids. Oxford Press, 2nd ed., pp. 58-60, 344-345.
3. Manohar, K., D. W. Yarbrough, and J. R. Booth. (2000). “Measurement of Apparent Thermal Conductivity by the Thermal Probe Method,” Journal of Testing and Evaluation, JTEVA, 28(5):345-351.
4. Ghuman, B. S., and R. Lal. (1985). “Thermal Conductivity, Thermal Diffusivity, and Thermal Capacity of Some Nigerian Siols,” Soil Science, 139(1):74-80.
5. Abu-Hamdah, N. H. (2000). “Effect of Tillage Treatments on Soil Thermal Conductivity of Sone Jordanian Clay Loam and Loam Siol,” Soil Tillage Research, 56:145-151.
6. American Society for Testing and Materials.(1995). “Standard Test Method for Determination of Thermal Conductivity of Soil and Soft Rock by Thermal Needle Probe Procedure,” Annual Book of ASTM Standards, ASTM D 5334:225-229.
7. Winterkorn, H. F.(1970). “Suggested Method of Test for Thermal Resistivity of Soil by the Thermal Probe,” Special Procedure for testing Soil and Rock for Engineering Purposes, ASTM STP 479:264-270.
8. Coleman, H. W., and W. G. Steller. (1999). “Experimentation and Uncertainty Analysis for Engineers,” 2<sup>nd</sup> ed., John Wiley and Sons, New York, pp. 47-64.

9. EXTECH Instruments. (2002). "Micro-Controller Based DC Power Supply," Instruction Manual, Bear Hill Road, Waltham, MA, USA.
10. Weast, R. C. (1982). CRC Handbook of Chemistry and Physics. CRC Press Inc., 62nd ed., p. E-82.
11. Kersten, M. S.(1949). "Thermal Properties of Soils," Bulletin of the University of Minnesota Institute of Technology, Engineering Experiment Station, LII(28).
12. Natrella, M. G.(1963). "Experimental Statistics," National Bureau of Standards Handbook, No. 91,
13. LaserComp FOX 304, "Heat Flow Meter Thermal Conductivity Instrument," Information Sheet, LaserComp, Wakefield, MA, USA.
14. Douglas, E. and E. McKyes. (1978). "Compaction Effects on the Hydraulic Conductivity of a Clay Soil," Soil Science, 125(5):278-282.
15. Avallone, E. A. and Baumeister, T. (1996). Marks' Standard Handbook for Mechanical Engineers, 10<sup>th</sup> ed., McGraw-Hill, New York, p. 4-83.

## **Thermal Conductivity of Trinidad ‘Guanapo Sharp Sand’**

Krishpersad Manohar, Lecturer, Mechanical and Manufacturing Engineering Department, The University of the West Indies, St. Augustine, Trinidad, West Indies. Email: [kmanohar@eng.uwi.tt](mailto:kmanohar@eng.uwi.tt)

Kimberly Ramroop, M.Phil. Candidate, Mechanical and Manufacturing Engineering Department, The University of the West Indies, St. Augustine, Trinidad, West Indies.

Gurmohan S. Kochhar, Professor, Department of Mechanical & Manufacturing Engineering, The University of the West Indies, St. Augustine, Trinidad, West Indies. Email: [guru@eng.uwi.tt](mailto:guru@eng.uwi.tt)

### **List of Figure Titles**

Figure 1 - Schematic of thermal probe

Figure 2 - Schematic of electrical circuit and data acquisition system

Figure 3 - Plot of Temperature-Time Variation of Probe Data for 1000 s

Figure 4 - Apparent Thermal Conductivity variation with wt.% Water for Sand Specimens

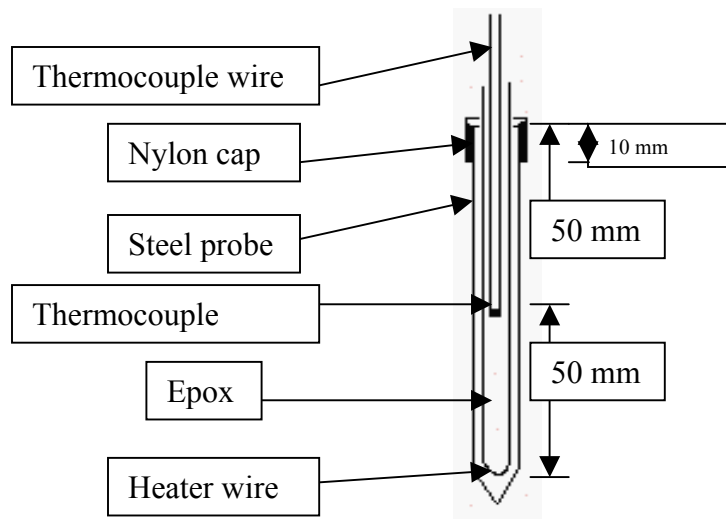


Figure 1 - Schematic of thermal probe

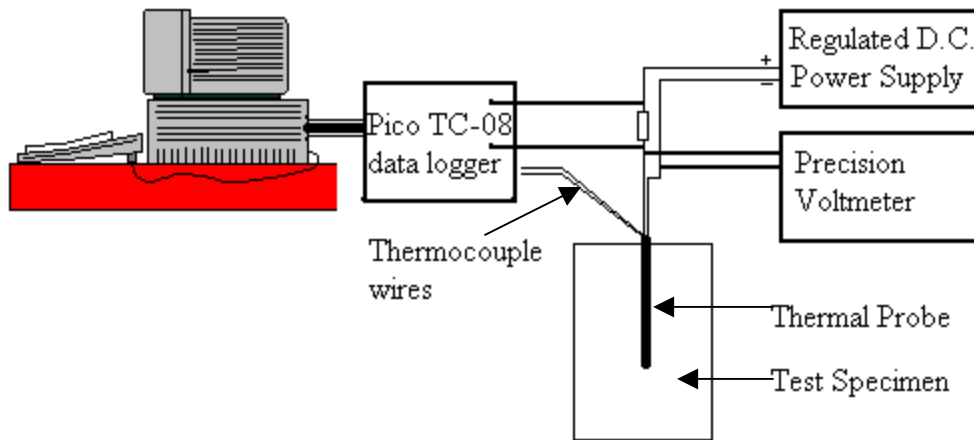


Figure 2 - Schematic of electrical circuit and data acquisition system

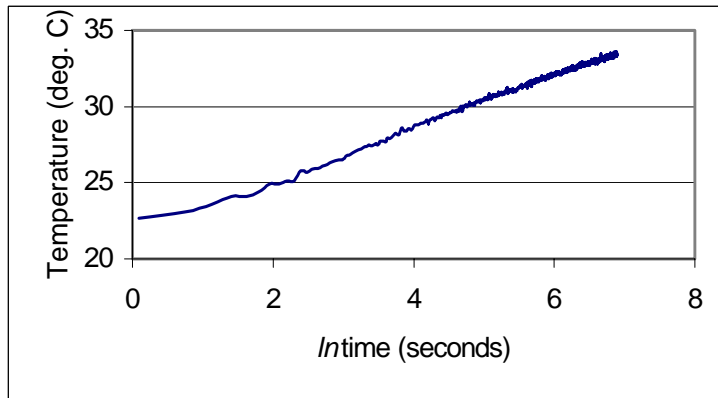


Figure 3 - Plot of Temperature-Time Variation of Probe Data for 1000 s

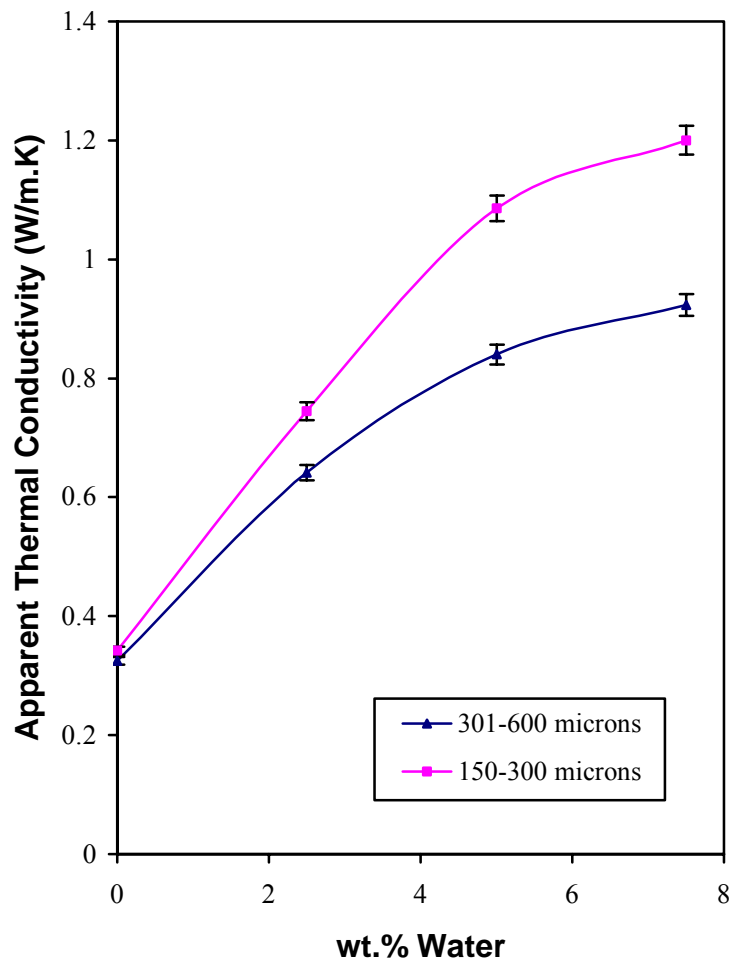


Figure 4 - Apparent Thermal Conductivity variation with wt.% Water for Sand Specimens